

# Application and Prospects of Molecular Imaging in Immunotherapy

This article was published in the following Dove Press journal:  
*Cancer Management and Research*

Weiqing Wang<sup>1,2</sup>  
Zhenhua Gao<sup>2</sup>  
Lu Wang<sup>2</sup>  
Jianing Li<sup>2</sup>  
Jinming Yu<sup>1,2</sup>  
Shumei Han<sup>2</sup>  
Xue Meng<sup>2</sup>

<sup>1</sup>School of Clinical Medicine, Weifang Medical University, Weifang, Shandong 261053, People's Republic of China;

<sup>2</sup>Department of Radiation Oncology, Shandong Cancer Hospital and Institute, Shandong First Medical University and Shandong Academy of Medical Sciences, Jinan 250117, Shandong, People's Republic of China

**Abstract:** Recently, immunotherapies that target the interactions of programmed cell death 1 (PD-1) with its major ligands, programmed death ligand 1 (PD-L1) and programmed death ligand 2 (PD-L2), have achieved significant success. To date, several immune checkpoint inhibitors targeting the PD-1/PD-L1 pathway have been developed to treat melanoma, non-small cell lung cancer, head and neck cancer, renal cell carcinoma, and urothelial carcinoma. Despite promising outcomes with immunotherapy, there are many limitations to several current immune biomarkers for predicting immune benefits and to traditional imaging for evaluating the efficacy and prognosis of immunotherapy and monitoring adverse reactions. In this review, we recommend a novel imaging method, molecular imaging. This paper reviews the application and prospects of molecular imaging in the context of current immunotherapies in regard to the following aspects: 1) detecting the expression of PD-1/PD-L1; 2) evaluating the efficacy of immunotherapy; 3) assessing patient prognosis with immunotherapy; 4) monitoring the toxicity of immunotherapy; and 5) other targets imaging.

**Keywords:** tumor, immunotherapy, PD-1, PD-L1, PET, SPECT

## Introduction

Despite therapies expanding, cancer remains one of the primary causes of mortality worldwide. Recently, immunotherapies that targets the interactions of programmed cell death 1 (PD-1) with its major ligands, programmed death ligand 1 (PD-L1) and programmed death ligand 2 (PD-L2), have achieved significant success.<sup>1</sup> PD-1 is expressed on the surface of activated T cells, B cells and natural killer cells.<sup>1-3</sup> PD-L1 is a surface glycoprotein ligand of PD-1. By binding to PD-1, PD-L1 leads to T cell response inhibition and cytotoxic T cell dysfunction. Through this mechanism, cancer cells can escape immune surveillance.<sup>4,5</sup> In 2014, the first anti-PD-1 antibody (Ab) was approved by the Food and Drug Administration (FDA) for advanced melanoma, and to date, several immune checkpoint inhibitors targeting the PD-1/PD-L1 pathway have been developed to treat melanoma, non-small cell lung cancer (NSCLC), head and neck cancer, renal cell carcinoma, and urothelial carcinoma.<sup>6-8</sup>

Despite the promise of immunotherapy, new problems have emerged in immunotherapy. 1) Immunotherapy is not only expensive but also only 20-40% patients show durable responses.<sup>9</sup> 2) Even though PD-L1, the tumor mutational burden (TMB), microsatellite instability (MSI) and deficient mismatch repair (dMMR) have been applied independently in the clinic,<sup>10-12</sup> due to the diversity of detection means, heterogeneity and dynamics,<sup>13-23</sup> some patients with high expression do not benefit from immunotherapy, whereas some patients with low expression may have

Correspondence: Xue Meng  
Department of Radiation Oncology,  
Shandong Cancer Hospital and Institute,  
Shandong First Medical University and  
Shandong Academy of Medical Sciences,  
Jinan 250117, Shandong, People's  
Republic of China  
Tel/Fax +86 0531-67627081  
Email mengxue123999@163.com

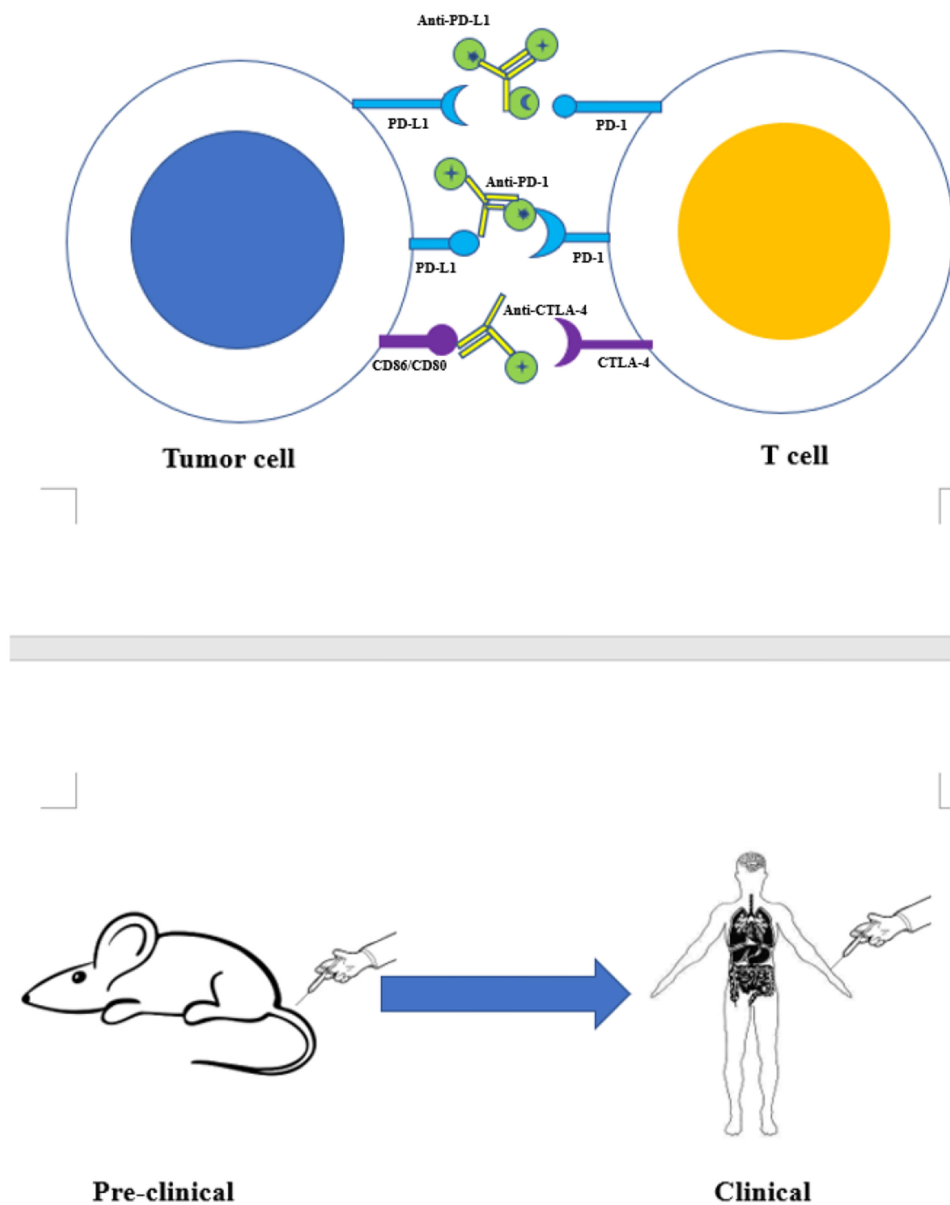


**Figure 1** Targeted molecular imaging of immune checkpoints from preclinical to clinical studies. Using radionuclide, fluorescent dye, or magnetic agent to label monoclonal antibodies as anti-PD-L1, anti-PD-1, anti-CTLA4 et al to form tracers. Injecting the tracer into the body of mice or patients for PET, SPECT, MRI, or optical imaging.

sustained response.<sup>24,25</sup> 3) Traditional imaging is not accurate in evaluating immune efficacy due to pseudoprogression<sup>26</sup> or hyperprogressive disease.<sup>27,28</sup> 4) Immunotherapy can result in a range of adverse effects, such as myocarditis, enterocolitis, and pneumonitis,<sup>29</sup> even leading to death. However, to date, there is no effective way to monitor these adverse reactions. Thus, there is an urgent need to identify a novel method to identify people who have a sustained response to immunotherapy, evaluate immunotherapeutic efficacy and prognosis, and monitor immunotoxicity. Molecular imaging has shown good potential in these areas. This paper reviews the application and

prospects of molecular imaging in the context of current immunotherapies in regard to the following aspects: 1) detecting the expression of PD-1/PD-L1; 2) evaluating the efficacy of immunotherapy; 3) assessing the prognosis of immunotherapy; and 4) monitoring the toxicity of immunotherapy; and 5) other targets imaging.

### Detection of the Expression of PD-1/PD-L1

Although it has been shown in clinical trials that patients with high PD-L1 expression have a sustained clinical response to immunotherapy,<sup>10</sup> there are many limitations. On the one hand, immunohistochemistry as the main

detection method of this biomarker has a variety of disadvantages, such as invasiveness, difficulty in collecting samples and inconsistency in positive criteria.<sup>13–15</sup> On the other hand, this expression is highly dynamic and heterogeneous.<sup>16–18</sup> Thus, some patients with positive expression do not benefit from immunotherapy; similarly, some patients with negative expression have a sustained clinical response.<sup>24,25</sup> Therefore, we need a noninvasive but more accurate detection method. Recently, many pre-clinical and clinical studies have demonstrated important advantages of positron emission tomography (PET), single-photon emission computed tomography (SPECT), Magnetic Resonance Imaging (MRI) and Optical imaging over immunohistochemistry in the detection of PD-1/PD-L1 expression.

### PET Imaging

In 2015, Natarajan et al developed the novel tracer <sup>64</sup>Cu-DOTA-PD-1 to detect PD-1 expression in transgenic mouse models of melanoma. This was the first report to show detection of the expression of PD-1 by PET imaging in vivo. The tracer showed obvious specificity for the tumor and related lymphoid organs: the tracer uptakes by tumor-infiltrating lymphocytes (TILs) in nonblocked and blocked mice were  $7.4 \pm 0.71\%$  and  $4.51 \pm 0.26\%$  (mean % ID/g  $\pm$  SD), respectively. The tracer uptake in clearance organs such as the liver and kidneys were  $16.09 \pm 3.72\%$  and  $5.61 \pm 3.37\%$  (% ID/g  $\pm$  SD), respectively, at 48 h.<sup>17</sup> In the same year, Maute et al used HAC-PD1 to develop a new tracer, <sup>64</sup>Cu-DOTA-HAC-PD1, which could be rapidly and specifically taken up by an hPD-L1 tumor. The study found higher uptake of the tracer in hPD-L1-positive cells ( $80.5 \pm 1.9\%$  ID/g) than in control hPD-L1-negative cells ( $8.3 \pm 0.1\%$  ID/g).<sup>30</sup> In 2016, Michael Hettich et al first attempted to use two tracers, <sup>64</sup>Cu-NOTA-PD-1 and <sup>64</sup>Cu-NOTA-PD-L1, for noninvasive imaging of both PD-1 and PD-L1 after immunotherapy combined with radiotherapy (RT). The results were consistent with the results of Natarajan et al; the expression of PD-1 and PD-L1 was mainly localized in the secondary lymphoid organs (spleen and lymph nodes).<sup>31</sup> Then, Lesniak et al used the tracer [<sup>64</sup>Cu] atezolizumab for PET imaging in SUM149 tumors, MDAMB231 tumors and CHO-hPD-L1 tumors. The results showed that tracer uptake increased from SUM149 tumors to MDAMB231 tumors and then CHO-hPD-L1 tumors ( $8.2 \pm 0.26$  and  $9.4 \pm 2.3$  VS  $10.8 \pm 0.4$  and  $17.2 \pm 2.1$  VS  $39.8 \pm 2.8$  and  $40.6 \pm 6.9\%$  ID/g at 24 h and 48 h, respectively), which was consistent with immunohistochemical results for the three

kinds of tumors (PD-L1 staining intensity increased according to the same pattern).<sup>32</sup> The study proved that [<sup>64</sup>Cu] atezolizumab could be used to detect PD-L1 expression in different tumor types. In 2017, England CG et al used the tracer <sup>89</sup>Zr-Df-pembrolizumab for PET imaging in a humanized mouse model. The study showed that the tracer accumulated in the liver and spleen ( $8.48 \pm 0.79\%$  ID/g and  $6.20 \pm 0.31\%$  ID/g, respectively). This was the first study to investigate the pharmacokinetics, biodistribution, and dosimetry of radiolabeled pembrolizumab in vivo. The study shows that <sup>89</sup>Zr-Df-pembrolizumab is appropriate for tracking the fate of pembrolizumab in vivo. Notably, PBL mice displayed high uptake in the salivary glands ( $11.13 \pm 0.82\%$  ID/g at 168 h).<sup>33</sup> Then, Chatterjee et al evaluated the highly specific PD-L1-binding peptide [<sup>64</sup>Cu] WL12 in in vivo and in vitro experiments and found that it could rapidly and specifically detect tumor expression of PD-L1.<sup>34</sup> Next, Mayer et al developed 3 radioactive tracer variants of HAC-PD-1 and used them for preclinical imaging and biological distribution studies to evaluate their ability to detect the expression of human PD-L1 in vivo. Among these, <sup>64</sup>Cu-NOTA-HAC-PD1 was best for detecting the expression of PD-L1 in vivo (region of interest (ROI)  $3.3 \pm 0.85\%$  ID/g). Notably, all HAC-PD1 radiotracer variants in this study enabled earlier detection of human PD-L1 expression than that previously reported.<sup>35</sup> The study showed that small, high-affinity engineered proteins such as HAC-PD1 have great potential in the clinical monitoring of PD-1 and PD-L1 expression to predict immune prognosis. In addition, Radiotherapy (RT) can induce upregulation of PD-L1 expression on tumor cells, which may affect the impact of PD-L1-based immunotherapy.<sup>36</sup> PD-L1 upregulation during radiotherapy is a dynamic process that has been difficult to monitor during treatment. In B16F10 tumor-bearing mice, Kikuchi et al used an <sup>89</sup>Zr-labeled anti-PD-L1 monoclonal antibody to monitor radiotherapy-induced PD-L1 upregulation. PET imaging showed that significant uptake of this tracer could be detected in neck tumors (irradiated, IR) relative to flank tumors (nonirradiated) (SUVmean  $1.5 \pm 0.18$  VS  $1.0 \pm 0.12$ ,  $p < 0.05$ ).<sup>37</sup> After, Kikuchi et al first used <sup>89</sup>Zr-nivolumab for PET imaging of nonhuman primates. The results indicated a specific biodistribution in the spleen. The success of this approach adds to the body of knowledge on the biological distributions of immunotherapeutic drugs in vivo.<sup>38</sup> In the same year, González Trotter et al radiolabeled the PD-L1-binding affibody molecule NOTA-ZPD-L1 1 with <sup>18</sup>F for PET imaging in PD-L1-positive, PD-L1-negative and mixed tumor-bearing mice.

PET imaging demonstrated high uptake of the tracer in the PD-L1-positive tumors but little tracer retention in the PD-L1-negative tumors. The kidneys ( $313 \pm 8\%$  injected dose per gram of tissue (ID/g)) and liver ( $0.98 \pm 0.10\%$  ID/g) in the PD-L1-positive tumor-bearing mice also showed high uptake of the tracer.<sup>39</sup> In 2018, Natarajan et al attempted to combine Cu with pembrolizumab for PET imaging in two different mouse models, one expressing hPD-1 in tumor cells (NSG/293 T/hPD-1) and the other lacking hPD-1 expression in tumor cells but containing some infiltrating TILs with hPD-1 expression (hNSG/A375). The study found that the uptake of the tracer was increased significantly in the tumors with high expression of PD-1. In addition, the PET signal in the TILs expressing hPD-1 was well contrasted with the PET signal in organs and background tissue removal.<sup>40</sup> At the same time, Charles Truillet et al developed a novel tracer  $^{89}\text{Zr-C4}$  for PET imaging to detect PD-L1 expression in vivo of male mice bearing H1975 xenografts (a PD-L1 positive model of human non-small-cell lung cancer bearing oncogenic EGFR L858R/T790M). The uptake of  $^{89}\text{Zr-C4}$  in the tumor was  $5\%$  ID/g and also 10-fold higher than the activity observed in blood pool, muscle, and bone, underscoring. The result showed a novel tracer  $^{89}\text{Zr-C4}$  can detect PD-L1 expression by PET imaging.<sup>41</sup> Then, Donnelly et al developed the  $^{18}\text{F-BMS-9,886,192}$  tracer for PET imaging in mice bearing bilateral PD-L1-negative and PD-L1-positive subcutaneous tumors. High uptake (3.5-fold) was observed in the PD-L1-positive subcutaneous tumors than in the PD-L1-negative tumors ( $2.41 \pm 0.29$  VS  $0.82 \pm 0.11\%$  ID/g,  $p < 0.0001$ ).<sup>42</sup> Next, Li et al used KN035 to develop the immuno-PET probe  $^{89}\text{Zr-Df-KN035}$ . In the study,  $^{89}\text{Zr-Df-KN035}$  uptake mainly occurred in mouse tumor tissue ( $18.08 \pm 2.34\%$  ID/g at 24 h) compared with other tissues, which was confirmed by pretreatment with unlabeled KN035.<sup>43</sup> In the same year, De Silva et al used a peptide-based imaging agent, [ $^{68}\text{Ga}$ ] WL12, to noninvasively detect PD-L1 expression in tumors by PET. Biodistribution studies showed a greater than 9-fold increase in [ $^{68}\text{Ga}$ ] WL12 accumulation in hPD-L1 tumors compared to control CHO tumors at all time points tested. The % ID/g values for hPD-L1 tumors were  $19.4 \pm 3.3$ ,  $11.56 \pm 3.18$  and  $9.89 \pm 1.72$  at 15, 60 and 120 min after injection, respectively. In contrast, control CHO tumors showed  $< 1.33 \pm 0.21\%$  ID/g uptake of [ $^{68}\text{Ga}$ ] WL12 at the same time points.<sup>44</sup> The study revealed the specificity of [ $^{68}\text{Ga}$ ] WL12 for detecting the expression of PD-L1. Subsequently, Moroz et al conducted a preclinical study that confirmed the feasibility of accurately measuring PD-

L1 expression in the tumor microenvironment using  $^{89}\text{Zr-atezolizumab}$ .<sup>45</sup> Meanwhile, Anna Moroz et al found that accumulation of  $^{89}\text{Zr-atezolizumab}$  and  $^{89}\text{Zr-C4}$  was equivalent in B16 F10 tumors ( $13.92 \pm 1.0$  VS  $13.83 \pm 0.5$  ID/g), while uptake of  $^{89}\text{Zr-atezolizumab}$  was significantly lower for PET imaging. The result showed using  $^{89}\text{Zr-C4}$  tracer by PET imaging may be simpler to measure PD-L1 expression.<sup>45</sup> Then, Niemeijer et al performed PET imaging with  $^{89}\text{Zr-nivolumab}$  in patients with NSCLC. The study showed that the tracer could feasibly detect PD-1 expression:  $^{89}\text{Zr-nivolumab}$  uptake was higher in patients whose tumor biopsy (s) showed aggregates of PD-1-positive tumor-infiltrating immune cells than in those whose biopsy (s) lacked aggregates (median SUV<sub>peak</sub> 7.0 vs 2.7,  $p = 0.03$ , Mann-Whitney U-test). They used the  $^{18}\text{F-BMS-9,886,192}$  tracer as well as to perform PET imaging in patients with NSCLC. Increased  $^{18}\text{F-BMS-986,192}$  uptake was observed in the biopsied tumor lesion of patients with a response compared with that of patients without a response (median standardized uptake value (SUV) peak: 4.3 VS 2.2). The results showed the feasibility of the tracer: tumor uptake was quantified. More importantly, the authors observed significant differences in tracer uptake among patients and among different tumor lesions within a patient. The tracer may be used to measure the heterogeneity of PD-L1 expression.<sup>46</sup> Later, Bensch et al performed molecular imaging in 25 patients with locally advanced or metastatic bladder cancer, NSCLC, or triple-negative breast cancer (TNBC). This was the first time that  $^{89}\text{Zr-atezolizumab}$  was evaluated in humans. The imaging signal was found to be consistent with the expression of PD-L1 in inflamed sites and various normal lymphoid tissues.<sup>47</sup> In 2019, Li et al used  $^{89}\text{Zr-Df-KN035}$  for PET imaging. They observed the downregulation of PD-L1 expression in a mouse model of NSCLC following gefitinib administration ( $4.73 \pm 1.58$  and  $0.73 \pm 0.71\%$  ID/g in the tumor before and after therapy, respectively).<sup>48</sup> Meanwhile, Ehlerding et al used by PET imaging to observe an increase in the expression of PD-L1 in H460 tumors following in vivo fractionated radiotherapy: the tumor uptake at 24 h postinjection was  $2.10 \pm 0.52\%$  ID/g in nonirradiated mice VS  $4.44 \pm 1.52\%$  ID/g in mice treated with 2 Gy x 5 fractions ( $p < 0.05$ ,  $n = 45$ ).<sup>49</sup> In 2020, Lv et al designed and developed a novel  $^{68}\text{Ga}$ -labeled nanometer tracer,  $^{68}\text{Ga-NOTA-Nb109}$ , for specific noninvasive imaging to detect PD-L1 expression in melanoma-bearing mouse models. The study result is consistent with that of De Silva et al, who found that the uptake of  $^{68}\text{Ga-NOTA-Nb109}$  by PD-L1

-positive cells was far greater than that by PD-L1-negative cells within 2 h ( $6.3 \pm 0.31$  VS  $1.3 \pm 0.44\%$  ID/g).<sup>50</sup> Next, Camilla Christensen et al developed the tracer  $^{89}\text{Zr}$ -DFO-6E11. In this study, the authors used this novel tracer to perform PET imaging of CT26 tumor-bearing mice treated with external irradiation (XRT) combined with PD-L1 blockade. The results showed that PET imaging could detect the dynamic expression of PD-L1: the tumor uptake increased from  $0.35 \pm 0.04\%$  ID/g in mice receiving no codose to  $3.07 \pm 0.15\%$  ID/g in mice receiving a 500  $\mu\text{g}$  codose.<sup>51</sup>

The study indicates that molecular imaging technology can dynamically monitor the expression of PD-L1 in the context of radiotherapy combined with immunotherapy, which would be helpful for choosing the right times to add immunotherapy and evaluate the efficacy of immunization.

### SPECT Imaging

In 2015, Heskamp et al observed the uptake of  $^{111}\text{In}$ -PD-L1. 3.1 in 5 breast cancer xenografts with different PD-L1 expression levels. The study showed that efficient uptake of  $^{111}\text{In}$ -PD-L1.3.1 was observed in tumors with high PD-L1 expression (mda-mb-231  $25.2 \pm 2.9\%$  ID/g at 3 days, sk-br-3  $22.0 \pm 5.1\%$  ID/g at 3 days), while no efficient accumulation was observed in tumors with undetectable PD-L1 expression (SUM149  $8.4 \pm 0.2\%$  ID/g at 3 days, BT474, McF-7  $10.0 \pm 0.7\%$  ID/g at 3 days).<sup>52</sup> This study was the first to demonstrate the feasibility of detecting PD-L1 expression in human xenograft tumors in immunodeficient mice using SPECT. In 2016, Josefsson et al developed a new tracer,  $^{111}\text{In}$ -DTPA-anti-PD-L1, for imaging and biodistribution studies in an immunocompetent mouse model of breast cancer.  $^{111}\text{In}$ -DTPA-anti-PD-L1 showed high signal intensity in tumors, the spleen and the thymus by SPECT imaging ( $29.5 \pm 7.4$ ,  $63.9 \pm 12.2$  and  $11.8 \pm 2.0\%$  ID/g).<sup>53</sup> Next, García et al labeled HYNIC tetrazine with  $^{99\text{m}}\text{Tc}$ , developing the tracer tri- $^{99\text{m}}\text{Tc}$ -HYNIC-TZ. The authors observed high uptake of the tracer by SPECT imaging. However, this tracer also accumulated in large quantities in normal tissues, such as the liver ( $14.15 \pm 0.43\%$  ID/g), intestines ( $5.62 \pm 0.59\%$  ID/g), and kidneys ( $7.84 \pm 1.63\%$  ID/g), at 1 h post injection.<sup>54</sup> In 2017, Nedrow et al developed a new tracer,  $^{111}\text{In}$ -DTPA-anti-PD-L1-BC, which not only further confirmed the conclusion of Josefsson et al, namely, that there was significant uptake of the tracer in the tumor and spleen ( $12 \pm 3.0$  and  $17 \pm 1.8\%$  ID/g at 24 h), but also determined an optimal imaging dose (3 mg/kg) in a mouse model of melanoma.<sup>55</sup> In 2019, Heskamp et al again performed SPECT imaging in a variety of tumor models after

successful imaging on 5 breast cancer xenografts with different PD-L1 expression levels in 2015. The study demonstrated the feasibility of SPECT imaging in detecting changes in PD-L1 expression during tumor radiotherapy: they observed significantly increased uptake of  $^{111}\text{In}$ -anti-mPD-L1 in irradiated CT26 tumors compared with nonirradiated tumors ( $26.3 \pm 2.0$  VS  $17.1 \pm 3.1\%$  ID/g,  $p=0.003$ ). A similar effect, although less pronounced, was observed for LLC1 cells ( $15.7 \pm 1.8$  VS  $12.3 \pm 1.7\%$  ID/g,  $p=0.033$ ).<sup>56</sup> Then the study by Qiu et al found better pharmacokinetics. They performed SPECT imaging experiments with [ $^{99\text{m}}\text{Tc}$ ] HYNIC-peg11-tz in H1975 and A549 tumor-bearing mice. Using this tracer for SPECT imaging could delineate H1975 tumors from normal tissue to produce high-contrast images.<sup>57</sup> In view of the feasibility of SPECT imaging with  $^{99\text{m}}\text{Tc}$  in preclinical studies, Xing et al followed conducting the first relevant early clinical study. They labeled anti-PD-L1-sdab with  $^{99\text{m}}\text{Tc}$  and performed SPECT/computed tomography (CT) imaging in NSCLC patients. A good biological distribution and image characteristics were observed in the NSCLC patients and proved that the tracer is feasible: 2-h primary T:BP ratios correlated with PD-L1 immunohistochemistry results ( $r=0.68$ ,  $p=0.014$ ). The 2-h T:BP ratio was lower in tumors with  $\leq 1\%$  PD-L1 expression than in those with high PD-L1 expression ( $1.89$  VS  $2.49$ ,  $p=0.048$ ).<sup>58</sup> These results show that SPECT imaging has strong potential to select the patients who are most likely to respond to immunotherapy. We can choose the right time to add immunotherapy by monitoring changes in PD-L1 expression during tumor radiotherapy.

### Optical Imaging

Optical imaging is promising approach to study the physiological changes at the molecular, cellular, and tissue levels. Optical imaging can be mainly divided into fluorescence imaging (FLI) and photoacoustic imaging (PAI). In 2016, Samit et al developed an imaging probe NIR-PD-L1-mAb to detect PD-L1 expression. They found higher fluorescence signal intensities with NIR-PD-L1-mAb in MDA-MB-231 tumors compared to SUM149 tumors ( $27\%$  VS  $0.1\%$  PD-L1-positive cells). In addition, increased fluorescence intensity was observed in liver and lungs. The study demonstrated that using NIR-PD-L1-mAb can specifically detect PD-L1 expression by fluorescent imaging.<sup>59</sup> In 2017, Du et al revealed the imaging probe PD-1-IRDye800CW exhibited a specific accumulation at the tumor region, 1.7-fold higher than the IgG control. The result further demonstrated the

feasibility that using PD-1-IRDye800CW to detect PD-L1 expression by fluorescence optical imaging.<sup>60</sup> PAI is usually used for local tissue imaging due to the higher resolution and tissue penetration depth. Liposome-based probes for PAI had been proven the feasibility to guide image tumors.<sup>61</sup> This emerging imaging method could be considered to apply to detect response of immunotherapy in the future.

### Optical and MRI Dual-Modality Imaging

Combinations may enhance sensitivity and specificity in terms of each imaging modality has specific merits and limitations. Du et al developed a novel theranostic nanoprobe PD-L1-PCI-Gd by dual-modality MRI and optical fluorescence imaging to detect PD-L1 expression in 4T1 and CT26 tumors. The study found that fluorescence at tumor sites was constantly 2.16-fold higher in PD-L1-targeted nanoparticles than the non-targeted control group at 4–48 h in 4T1 tumors. Similar trends were observed by in CT26 tumors that the ratio was around 1.98-fold higher from 6 h to 48 h. The study also found that images obtained pre-contrast exhibited significantly increased 24h post-injection of PD-L1-PCI-Gd by MRI imaging in 4T1 and CT26 tumors compared with the non-targeted control group, around 1.50 and 1.61-fold respectively. This is the first report of cerasomes targeted to PD-L1 as agents for dual modality imaging and antitumor therapy. The study showed that using PD-L1-PCI-Gd for MRI/NIRF dual-mode imaging may help detect PD-L1 expression.<sup>62</sup>

Compared with PET/CT, SPECT/CT has better resolution, and SPECT imaging is less expensive and more common in the preclinical setting. However, in clinical applications, the resolution, sensitivity, and quantification of PET/CT are superior to those of SPECT/CT. In these two imaging approaches, many radioisotopes have been used to label ligands to form various tracers. However, the half-life of each radionuclide is different: <sup>18</sup>F has a half-life of 109 m, <sup>64</sup>Cu has a half-life of 12.7 h, <sup>68</sup>Ga has a half-life of 1.1 h, <sup>89</sup>Zr has a half-life of 78.4 h, and <sup>99m</sup>Tc has a half-life of 6 h. Now, commonly used tracers, on the one hand, are formed by using a radionuclide to label antibodies. The tracers need to use an isotope with a long half-life, such as <sup>111</sup>In, <sup>89</sup>Zr, or <sup>64</sup>Cu, for labelling. The isotope can match the antibody imaging time required and allow high-contrast imaging. However, isotopes with a long half-life have many disadvantages, such as a slowed clearance rate, long imaging time and high radiation dose to healthy organs.

Therefore, they are not suitable for clinical application. On the other hand, some scholars have turned their attention toward smaller radionuclide-tagged ligands, such as connection proteins in fluid molecules and peptides. The radionuclide labels these small molecular ligands to form tracers. These tracers have the characteristics of a fast clearance rate, strong specificity, high stability and fast tumor absorption, which are more conducive to clinical application. If we consider HAC-PD1 as an example, although changes in the metal from copper to gallium may alter the binding affinity, the uptake of <sup>64</sup>Cu-NOTA-HAC-PD1 and <sup>68</sup>Ga-NOTA-HAC-PD1 in almost identical hPD-L1 tumors shows similar affinities (ROI 3.3 ± 0.85 VS 3.8 ± 1.6% ID/g). However, compared with that of <sup>64</sup>Cu, the liver signal of <sup>68</sup>Ga is significantly reduced (17.0 ± 5.9 VS 8.1 ± 0.2% ID/g).<sup>35</sup> <sup>68</sup>Ga is easy to produce and less expensive than <sup>64</sup>Cu. Similarly, WL12 can be combined with copper or gallium to form tracers and shows similar affinities for uptake in an hPD-L1 tumor model.<sup>34,44,50</sup>

However, these tracers are currently applied only in the preclinical setting, but it is undeniable that the tracers have good application prospects to detect PD1/PD-L1 expression in clinical practice. And optical imaging (FLI and PAI) is relatively safer and sensitivity than nuclear imaging as an emerging approach to detect PD1/PD-L1 expression. Based on each imaging modality has specific merits and limitations, combinations may have better prospects such as PD-L1-PCI-Gd for MRI/NIRF dual-mode imaging.<sup>62</sup> In addition, Du et al showed the potential for the diagnosis and treatment of breast tumors of IRDye800CW and <sup>64</sup>Cu-labeled anti-PD-1 mAb-targeted Liposome-DOX by fluorescence and PET imaging.<sup>63</sup>

### Evaluation of the Efficacy of Immunotherapy

In terms of evaluating the efficacy of immunotherapy, Tazdait et al found that conventional Response Evaluation Criteria in Solid Tumors (RECIST) 1.1 underestimated the benefit of PD-1 or PD-L1 inhibitor therapy in approximately 11% of the evaluated population.<sup>64</sup> Wolchok et al first proposed the new immune-related response criteria iRECIST in 2009.<sup>65</sup> Even though the new standards improved accuracy by 4–8%,<sup>66–68</sup> they were still based on changes in tumor size seen with anatomical imaging modalities to evaluate the efficacy of immunotherapy.<sup>69–71</sup> Thus, these criteria still underestimated the immune

benefits due to the presence of atypical responses, such as pseudoprogression<sup>26</sup> and hyperprogressive disease.<sup>27,28</sup>

In the sequence of complex metabolic and functional processes that occur during and after treatment, evaluating the efficacy of immunotherapy by monitoring tumor size changes is one approach. However, <sup>18</sup>F-FDG PET, as an indicator for intracellular glucose metabolism, is a modality that can be used to detect metabolic changes before anatomical changes occur. Therefore, Wall et al proposed PET Response Criteria in Solid Tumors version 1.0 (PERCIST) instead of RECIST to assess the treatment response.<sup>72</sup> A prospective study by Beer et al found that two patients (5%) among 42 patients treated with a PD-1/PD-L1 inhibitor were classified as having pseudoprogression by <sup>18</sup>F-FDG PET/CT. Interestingly, the sum of diameters increased by 2040% at the first follow-up compared with the baseline, and the SUV normalized by lean body mass (SUL) peaks of both lesions decreased by 13% and 16%, respectively, at the first follow-up, followed by complete resolution.<sup>73</sup> Kaira et al performed the first prospective study to investigate the clinical significance of <sup>18</sup>F-FDG accumulation on PET/CT scans in patients with advanced NSCLC who received nivolumab. They found that the predictive probabilities of a partial response (PR; 100% VS 28.6%,  $p = 0.021$ ) and progressive disease (PD; 100% VS 22.2%,  $p = 0.002$ ) confirmed with RECIST at 1 month after nivolumab initiation were significantly higher in total lesion glycolysis (TLG) by PET imaging than by CT imaging.<sup>74</sup> A prospective study by Cho et al used <sup>18</sup>F-FDG PET/CT to evaluate the effect of immunotherapy on twenty patients with advanced melanoma receiving immunotherapy. They found that the optimal PERCIST and European Organisation for Research and Treatment of Cancer (EORTC) threshold values predictive of the best overall response were  $>15.5\%$  and  $>14.7\%$ , respectively, indicating that increased FDG tumor uptake between 21 and 28 days on therapy may correlate with eventual clinical benefit.<sup>75</sup> In addition, Higuchi et al found decreased FDG uptake in each recurrent lesion of a 75-year-old man with metastatic NSCLC on six courses of nivolumab treatment; in particular, the SUVmax of the supraclavicular lymph node and disseminated lesions before and after immunotherapy decreased from 9.8 to no accumulation and 5.9 to 3.4, respectively.<sup>76</sup> These results suggest the potential value of FDG PET in monitoring the response to this immunotherapy. <sup>18</sup>F-FDG PET imaging could be helpful in distinguishing between patients with true PD and those with a transient increase in tumor volume followed by a response to therapy.

The study confirmed that as PD1/PD-L1 expression in patients increased, the probability of benefitting from immunotherapy became higher.<sup>10</sup> A large number of pre-clinical studies have shown that the uptake of tracers formed by using a radioactive nuclide to label an antibody is high in tumors with high PD-1/PD-L1 expression. This possibly allows researchers to use longitudinal observation of tracer uptake to evaluate immune efficacy.

## Assessing the Prognosis of Immunotherapy

In an article by Sachpekidis et al, <sup>18</sup>F-FDG PET was used to evaluate tumor response after ipilimumab treatment administration for more than one cycle according to the EORTC 1999 criteria. Patients were divided into two groups by SUV changes. An increase in the SUV  $>25\%$  was deemed to indicate progressive metabolic disease (PMD), and an increase in the SUV  $<25\%$  or a decrease in the SUV  $<15\%$  was considered to indicate stable metabolic disease (SMD). The study found that the progression-free survival (PFS) of the patients with SMD was significantly longer than that of the patients who were deemed to have PMD (9.8 VS 3.6 months,  $P < 0.001$ ).<sup>77</sup> Kaira et al found that all patients achieving a partial metabolic response (PMR) by TLG were able to continue nivolumab treatment for more than 5 months without recurrence, whereas those with PMD by TLG acquired resistance to nivolumab within approximately 3.5 months.<sup>74</sup> Cho et al suggested the use of PET/CT Criteria for early prediction of Response to Immune checkpoint inhibitor Therapy (PECRIT), a combination of functional and anatomical parameters obtained by PET/CT 3 to 4 weeks after therapy onset for early prediction of an eventual response to immunotherapy. According to the study, in patients with stable disease (SD) by RECIST1.1 at 3 to 4 weeks, an increase  $> 15.5\%$  in the SUL peak of the hottest lesion by <sup>18</sup>F-FDG PET/CT was associated with eventual clinical benefit (a PR or complete response (CR) at 4 months or SD  $\geq 6$  months).<sup>75</sup> Tan et al performed <sup>18</sup>F-FDG PET imaging in metastatic melanoma patients treated with anti-PD-1 therapy. They found that in 78 complete metabolic response (CMR) patients, 78% had discontinued treatment, but almost all these patients remained progression free at 1 year.<sup>78</sup> Ito et al found that in responders and nonresponders receiving ipilimumab therapy, the two-year overall survival (OS) rate was 66% VS 29% for imPERCIST5

( $p=0.003$ ). The authors also compared the prognosis of patients with PMD and SMD (and responders with non-responders). PFS was significantly longer for the patients with disease stabilization (9.8 months VS 3.6 months,  $p < 0.001$ ).<sup>79</sup> They also found that when the  $^{18}\text{F}$ -FDG PET/CT parameter wMTV was higher than the cut-off value of  $27 \text{ cm}^3$ , 142 consecutive patients with melanoma treated with single-agent ipilimumab therapy had a significantly shortened median OS time (26 months VS 10.8 months).<sup>80</sup> Similarly, Giovanni Rossi et al found that 15 to 23% of PMR patients receiving nivolumab therapy were defined as having SD or even PD by RECIST or immune-related response criteria (irRC) but all these patients were still alive at 12 months. Compared with CT-based evaluation criteria, the evaluation criteria for immunity based on PET showed better OS.<sup>81</sup> Next, Annovazzi et al conducted a retrospective study that involved  $^{18}\text{F}$ -FDG PET/CT imaging in fifty-seven patients with metastatic melanoma treated with ipilimumab ( $n = 25$ ; group 1) or with PD-1 inhibitors ( $n = 32$ ; group 2). They found a high PFS rate at 1 year in responders identified by MTV and TLG (group 1, 90.80% of patients were progression free at 1 year; group 2, 100.100%).<sup>82</sup> Dercle et al found a significantly increased  $^{18}\text{F}$ -FDG uptake SUVmax in the spleen of responders receiving anti-PD1 treatment. This shows that increased uptake may be associated with a favorable prognosis.<sup>83</sup> Here, we confirmed the prognostic value of  $^{18}\text{F}$ -FDG PET/CT, opening a new prognostic window for patients treated with immunotherapy.

In addition, Lim et al found that relatively high NaF SUVmax values were associated with worse OS in patients with advanced genitourinary malignancies treated with cabozantinib and nivolumab with or without ipilimumab.<sup>84</sup>

In terms of tracers created with other elements, Bensch et al found that uptake of the tracer  $^{89}\text{Zr}$ -atezolizumab appeared to be a strong predictor of response to atezolizumab therapy, including prolonged PFS and OS. They found that patients with below-median uptake (SUVmax geom. mean  $< 9.0$ ) were more likely to progress or die than those with above-median uptake (SUVmax geom. mean  $\geq 9.0$ ).<sup>47</sup>

These results fully demonstrated the potential of molecular imaging for assessing the prognosis of immunotherapy.

## Monitoring the Toxicity of Immunotherapy

Immunotherapy, which affects not only the cancer being targeted but also any sensitive healthy tissue, can have a range of adverse effects, such as maculopapular rash,

enterocolitis, dysthyroidism, pneumonitis, and hepatitis.<sup>29</sup> Although most adverse effects are low intensity, approximately 10% of patients treated with immune checkpoint inhibitors will develop severe adverse effects<sup>85</sup> that can even be life-threatening. A meta-analysis by Daniel Y. Wang showed that the toxicity-related fatality rates were 0.36% (anti-PD-1 therapy), 0.38% (anti-PD-L1 therapy), 1.08% (anti-CTLA-4 therapy), and 1.23% (anti-PD-1/PD-L1 plus anti-CTLA-4 therapy) in 19,217 patients in 112 trials.<sup>86</sup> Therefore, immunotoxicity should be fully considered. However, there are still great limitations in detecting immunotoxicity. 1) Due to the continuous emergence and development of the concept of adverse reactions, clinicians may lack a good understanding of the concept of immune-related adverse reactions. 2) In addition, many fatal complications have occurred in the early stage of treatment, and different treatment plans are needed for different complications, which requires clinicians to identify these complications as early as possible and address them in a timely manner. 3) Furthermore, adverse effects include various entities and involve different organs, which leads to the need for different imaging methods to detect these adverse reactions.<sup>87</sup> 4) Finally, adverse reactions can masquerade as a variety of conditions. For example, Jeffrey S Weber et al found that inflammation in target lesions might be misinterpreted as progression when a so-called tumor flare reaction appears.<sup>88</sup> These complications can be delayed: adverse effects may occur during treatment, at the time of discontinuation, or even months after immunotherapy.<sup>27</sup> Misdiagnosis of adverse events, such as infection or progression of disease, may very well turn a potentially easily treatable condition into a life-threatening complication.

In a retrospective case series study, high uptake of F-18 FDG observed by PET-CT imaging was found in the pancreas, ascending colon, pituitary gland and thyroid gland of four patients with melanoma treated with ipilimumab. Ultimately, one patient had confirmed immune-mediated pancreatitis, one had colitis, one had hypophysitis, and one had confirmed thyroiditis.<sup>89</sup> Similarly, Dercle et al found that by  $^{18}\text{F}$ -FDG PET imaging, 37% of patients had new nontumor lesions related to immune side effects during anti-PD1 treatment (one confirmed colitis case, two interstitial pneumonitis cases and one confirmed pancreatitis case).<sup>75</sup> In addition, we mentioned that colitis is a common side effect of immunotherapy. In the colon, PD-L1 upregulation is involved in the regulation of chronic inflammation in the colonic mucosa.<sup>90</sup> Therefore, when



we use immunotherapy, we can monitor the expression of PD-L1 through molecular imaging to avoid the occurrence of irreversible colitis.

These studies indicate the feasibility of molecular imaging in detecting and even predicting adverse immune reactions.

## Other Targets Imaging

### CTLA-4

As a transmembrane inhibitory receptor, cytotoxic T lymphocyte-associated antigen-4 (CTLA-4) is expressed on activated T lymphocytes, including activated T-cells, memory T-cells, and T reg -cells.<sup>91</sup> CTLA-4 suppressed T cell-mediated immune responses. Through this mechanism, CTLA-4 can lead to the development of Tumors.<sup>4</sup> In 2011, ipilimumab, an anti-CTLA-4, was approved by the FDA for the treatment of melanoma.

Initially, Higashikawa et al developed a molecular imaging probe <sup>64</sup>Cu-DOTA-anti-CTLA-4 mAb for imaging CTLA-4-expressing TILs in CT26 tumors. The study found that <sup>64</sup>Cu-DOTA-anti-CTLA-4 mAb showed higher accumulation than control groups in the tumors (SUV-max:2.65 ±0.01 VS 2.06±0.32).<sup>92</sup> In 2017, Ehlerding et al evaluated the biodistribution of <sup>64</sup>Cu-DOTA-ipilimumab using PET imaging in CTLA-4 expressing lung cancer xenografts mice bearing. High accumulation of <sup>64</sup>Cu-DOTA-ipilimumab was found in CTLA-4-expressing tumor cells (A549 cells 9.5 ± 2.4%, H460 cells 7.6 ± 1.2% and the H358 cells 4.6± 1.3% ID/g). Ipilimumab was found to bind to the CTLA-4-expressing lung cancer xenografts cells.<sup>93</sup> In 2019, Ehlerding et al developed two tracers <sup>64</sup>Cu-NOTA-ipilimumab and <sup>64</sup>Cu-NOTA-ipilimumab-F(ab')<sub>2</sub> by PET imaging, providing a means to to localize CTLA-4+ T-cells in humanized mouse models. The highest accumulation of <sup>64</sup>Cu-NOTA-ipilimumab was observed, peaking at 7.00 ± 2.19%ID/g in the salivary glands of PBL mice. In contrast, <sup>64</sup>Cu-NOTA-ipilimumab-F(ab')<sub>2</sub> uptake was 2.40 ± 0.86%ID/g at the same time point. However, the F(ab')<sub>2</sub> agent cleared from circulation more quickly than <sup>64</sup>Cu-NOTA-ipilimumab, providing higher salivary gland-to-blood ratios (1.78 ± 0.72 VS 1.19 ± 0.49 at 48 h). The study showed using <sup>64</sup>Cu-NOTA-ipilimumab and <sup>64</sup>Cu-NOTA-ipilimumab-F(ab')<sub>2</sub> for PET imaging was able to noninvasively track CTLA-4+ tissues. These tracers may help elucidate the response of CTLA-4-targeted checkpoint in immunotherapy treatments.<sup>94</sup>

### Granzyme B

Granzyme B is a serine protease by active tumoral cytotoxic T cells releasing. The immune synapses bind to the

tumor cells and release granzymes, perforins, granzylins to the synaptic cleft. Through this mechanism, Granzylins and perforins result in the apoptosis of tumor cells.<sup>95</sup>

Larimer et al provided a preclinical proof of concept that granzyme B as a reliable early-response biomarker, the expression of which is high in immunotherapy. They developed a human probe <sup>68</sup>Ga-NOTA-GZP by PET imaging to detect granzyme B expression in CT26 tumor. They found that the highest uptake of <sup>68</sup>Ga-NOTA-GZP in tumor with combination treatment of anti-CTLA-4 and anti-PD-1 antibodies, compared to mono immune checkpoint therapy and untreated mice (TBR = 1.83±0.18 VS 1.29±0.12 VS 0.96 ±0.11). The study proved that the <sup>68</sup>Ga-NOTA-GZP for PET imaging may serve as a noninvasive imaging means to Identify the responders for immunotherapy.<sup>96</sup>

### IFN-Gamma

The cytokine interferon-γ (IFN-γ) is predominantly produced by activated skewed CD4 T cells and cytotoxic CD8 T cells which contribute to antigen-specific tumor cell recognition and destruction in immunotherapy (100–103).<sup>97–100</sup> IFN-γ signaling can upregulate the Fas/FasL and MHC molecules to kill tumor cell (104,105)<sup>101,102</sup> and regulate tumor expression of PD-L1 to quell immune activation.

In 2018, Gibson et al developed the tracer <sup>89</sup>Zr-anti-IFN-γ for PET imaging in BALB/c mice. They found that high tracer uptake in the tumor compared with liver and blood at 72 h by PET imaging. And a nearly two-fold increase in tumor uptake was observed in vaccinated compared with control mice (10.07 ±1.50% VS 5.97 ± 0.61% ID/g, p=0.0001). It showed the feasibility of the tracer as a non-invasive measure to identify production and function of IFN-γ in immunotherapy.<sup>103</sup>

### CD4 and CD8

Increasing evidence suggests that the CD4 + and CD8 + lymphocytes in the tumor microenvironment of patients are important for initiating and mediating a response to immunotherapy.<sup>104–109</sup> Therefore, the ability to non-invasively visualize CD4+ and CD8+ T cells in vivo would play a critical role during immunotherapy.

In 2014, Tavaré et al used engineered antibody fragments for PET imaging of CD8 + T cells. They found that the uptake of <sup>64</sup>Cu-NOTA-2.43 Mb by PET imaging was higher five to ninefold in the spleen, lymph nodes of the antigen-positive B/6 mice compared with antigen-negative Lyt2.1 C3H mice (75 ±8.5% VS 15 ± 2.3%ID/g, 27 ±7.9%

D/g VS  $2.7 \pm 0.71\%$ ID/g respectively). The study showed the feasibility of using PET imaging to detect CD8 expression.<sup>110</sup> In 2015, Tavaré et al further found that CD4 and CD8 T cell populations in vivo were targeted and visualized in the spleen and lymph nodes of wild-type mice. The study showed potential applications that using the <sup>89</sup>Zr-radiolabeled anti-CD4 and -CD8 cDbs by PET to monitor response of immune cell subsets in immunotherapy.<sup>111</sup> In 2016, Tavaré et al used the <sup>89</sup>Zr-malDFO-169 cDb further validated the feasibility to detect changes of CD8 expression in preclinical tumor immunotherapy models.<sup>112</sup> In 2019, Kristensen et al developed tracers <sup>89</sup>Zr-DFO-CD4/<sup>89</sup>Zr-DFO-CD8a by PET imaging to detect and assess CD4 + and CD8a + status in CT26 tumor-bearing mice.<sup>113</sup> In 2020, Pandit-Taskar et al used the <sup>89</sup>Zr-IAB22M2C by PET imaging to carry out a prospective Phase I, open-label, non-randomized, dose escalation imaging study in malignant tumor patients receiving immunotherapy. The study found that the notably high uptake of <sup>89</sup>Zr-IAB22M2C in targeting CD8+ T cell-enriched tissues such as spleen, bone marrow, lymph nodes and tumors by directed imaging of CD8+ T cells. This was the first-in-human study of <sup>89</sup>Zr-IAB22M2C by PET imaging. It showed the <sup>89</sup>Zr-IAB22M2C is safe, feasible, and well tolerated to detect the CD8+ T cell accumulation within tumors.<sup>114</sup>

### OX40

CD134, TNFRSF4 (OX40) as a member of the tumor necrosis factor (TNF) receptor superfamily, binds the ligand CD252, TNFSF4 (OX40L) on activated antigen presenting cells (APCs), leading to recruitment of TNF-receptor associated factors (TRAFs), formation of a T cell receptor (TCR)-independent signaling complex and downstream activation of NF-kappaB.<sup>115</sup> Through this mechanism, it can produce cytokines such as IL-2 and IFN- $\gamma$  to promote T cells survival, proliferation and activation.

In 2018, Alam et al showed that the tracer <sup>64</sup>Cu-DOTA-AbOX40 by PET imaging was used to image OX40 noninvasively and longitudinally. The pronounced <sup>64</sup>Cu-DOTA-AbOX40 signal was observed in the TDLN of dual A20 lymphoma-tumor bearing mice, receiving either an immune stimulant (Cytosine phosphodiester Guanin-oligodeoxynucleotides (CpG-ODN), microbial signature DNA fragments) or vehicle only intratumorally in one tumor, the second tumor was untreated, at 24 hours after tracer injection. Furthermore, the tracers were signally accumulated in the tumor draining lymph node (TDLN)

and spleen (247.9%,  $p < 0.0001$ ) at day 9 post treatment. The study demonstrated that anti-OX40 Abs were suitable for PET imaging of activated T cells in vivo.<sup>116</sup>

In addition, in 2019, there are many NOD ligands having been synthesized in terms of the cytosolic nucleotide-binding oligomerization domains 1 and 2 (NOD1 and NOD2) receptors. The NOD2 agonists especially showed exhibit favorable immunostimulatory and anticancer activity.<sup>117</sup> Next, Kapp et al developed a novel family of L-nucleotide-protected TLR9 agonists EnanDIM which had been proven potential in immunotherapy.<sup>118</sup> In the future, the imaging of nucleotide aspect is something to looking forward to.

### Challenges and Future Directions

Until now, a lot of immune checkpoint inhibitors have been developed and applied for tumor treatment. Despite the promise of immunotherapy, Immunotherapy is not only expensive but also only 20-40% patients show durable responses. Although, we have proven molecular imaging has shown good potential in screening patients beneficiaries, evaluating the efficacy and prognosis of immunotherapy. However, we face many challenges: 1) Only a fraction of receptors and ligands inhibiting immune responses have been identified and imaged. In the future, we need find more targets for imaging by exploring and monitoring mechanism and response of immunotherapy. 2) Due to disadvantages of existing tracer for molecular imaging, in the future, we need to develop a safe, high-sensitivity and high-specificity tracer with stable expression in the human body that can distinguish between cancer and immune cells in the lymphoid organs and also accurately detect targets expression such PD-L1. 3) There is a lack of clinical trials. To date, most tracers have been evaluated only in preclinical studies, and we lack enough clinical data to further confirm the clinical safety of molecular imaging technology and the feasibility of predicting patients who benefit from immunotherapy and monitoring immune efficacy. 4) There is a lack of related laboratories. 5) Although, the existing PET and SPECT imaging or emerging MRI and optical imaging have showed good potential in immunotherapy. However, each imaging modality has specific merits and limitations. Based on the good prospects of dual-mode imaging for the diagnosis and treatment of tumors or detecting PD-L1 expression et al, combination of imaging technologies may be a major direction in the future.

In conclusion, despite these deficiencies, it is undeniable that molecular imaging has good application prospects in predicting immune benefits, evaluating immune efficacy and prognosis and even monitoring immunotoxicity.

## Conclusion

In this article, due to the many limitations of several current immune biomarkers in predicting immune benefits and those of traditional imaging in evaluating the efficacy and prognosis of immunotherapy and monitoring adverse reactions, we recommend a novel imaging method, molecular imaging.

This article summarizes the good application prospects of molecular imaging in screening patients who benefit from immunotherapy, evaluating the efficacy of immunotherapy, assessing treatment prognosis and monitoring adverse immune reactions. However, at present, molecular imaging technology has not been widely applied in clinical practice due to the difficulty of developing suitable tracers, the absence of clinical trials and the limitations of the current state of the technology. However, molecular imaging is undeniably a hotspot for future research. As this series of problems is solved, molecular imaging will eventually become an effective means for predicting patients who benefit from immunotherapy, evaluating the efficacy and prognosis of immunotherapy, and even monitoring immunotoxicity.

## Acknowledgments

The authors would such as to express their great thanks to the Academic Promotion Program of the Shandong First Medical University.

## Author Contributions

All authors made substantial contributions to conception and design, acquisition of data, or analysis and interpretation of data; took part in drafting the article or revising it critically for important intellectual content; agreed to submit to the current journal; gave final approval of the version to be published; and agree to be accountable for all aspects of the work.

## Funding

National Natural Science Foundation of China (81972864). Science and Technology Support Plan for Youth Innovation Teams of Universities in Shandong Province (2019KJL001). Science and Technology Plan of

Jinan (201907113). Academic Promotion Program of Shandong First Medical University (2019RC002).

## Disclosure

The authors declare that they have no competing interests for this work.

## References

- Riella LV, Paterson AM, Sharpe AH, Chandraker A. Role of the PD-1 pathway in the immune response. *Am J Transplant.* 2012;12:2575–2587. doi:10.1111/j.1600-6143.2012.04224.x
- Terme M, Ullrich E, Aymeric L, et al. IL-18 induces PD-1-dependent immunosuppression in cancer. *Cancer Res.* 2011;71:5393–5399. doi:10.1158/0008-5472.CAN-11-0993
- Fanoni D, Tavecchio S, Recalcati S, et al. New monoclonal antibodies against B-cell antigens: possible new strategies for diagnosis of primary cutaneous B-cell lymphomas. *Immunol Lett.* 2011;134:157–160. doi:10.1016/j.imlet.2010.09.022
- Pardoll DM. The blockade of immune checkpoints in cancer immunotherapy. *Nat Rev Cancer.* 2012;12:252–264. doi:10.1038/nrc3239
- Freeman GJ, Long AJ, Iwai Y, et al. Engagement of the PD-1 immunoinhibitory receptor by a novel B7 family member leads to negative regulation of lymphocyte activation. *J Exp Med.* 2000;192:1027–1034. doi:10.1084/jem.192.7.1027
- Home - ClinicalTrials.gov.; 2020. Please delete the reference 6
- Gong J, Chehrizi-Raffle A, Reddi S, Salgia R. Development of PD-1 and PD-L1 inhibitors as a form of cancer immunotherapy: a comprehensive review of registration trials and future considerations. *J Immunother Cancer.* 2018;6:8.
- Zhan MM, Hu XQ, Liu XX, Ruan BF, Xu J, Liao C. From monoclonal antibodies to small molecules: the development of inhibitors targeting the PD-1/PD-L1 pathway. *Drug Discov Today.* 2016;21:1027–1036.
- Sharma P, Allison JP. The future of immune checkpoint therapy. *Science.* 2015;348:56–61. doi:10.1126/science.aaa8172
- Mok T, Wu YL, Kudaba I, et al. Pembrolizumab versus chemotherapy for previously untreated, PD-L1-expressing, locally advanced or metastatic non-small-cell lung cancer (KEYNOTE-042): a randomised, open-label, controlled, Phase 3 trial. *Lancet.* 2019;393:1819–1830. doi:10.1016/S0140-6736(18)32409-7
- Overman MJ, McDermott R, Leach JL, et al. Nivolumab in patients with metastatic DNA mismatch repair-deficient or microsatellite instability-high colorectal cancer (CheckMate 142): an open-label, multicentre, Phase 2 study. *Lancet Oncol.* 2017;18:1182–1191. doi:10.1016/S1470-2045(17)30422-9
- Ott PA, Bang YJ, Piha-Paul SA, et al. T-cell-inflamed gene-expression profile, programmed death ligand 1 expression, and tumor mutational burden predict efficacy in patients treated with pembrolizumab across 20 cancers: KEYNOTE-028. *J Clin Oncol.* 2019;37:318–327. doi:10.1200/JCO.2018.78.2276
- Meng X, Huang Z, Teng F, Xing L, Yu J. Predictive biomarkers in PD-1/PD-L1 checkpoint blockade immunotherapy. *Cancer Treat Rev.* 2015;41:868–876. doi:10.1016/j.ctrv.2015.11.001
- Topalian SL, Taube JM, Anders RA, Pardoll DM. Mechanism-driven biomarkers to guide immune checkpoint blockade in cancer therapy. *Nat Rev Cancer.* 2016;16:275–287. doi:10.1038/nrc.2016.36
- Patel SP, Kurzrock R. PD-L1 expression as a predictive biomarker in cancer immunotherapy. *Mol Cancer Ther.* 2015;14:847–856. doi:10.1158/1535-7163.MCT-14-0983
- Taube JM, Anders RA, Young GD, et al. Colocalization of inflammatory response with B7-h1 expression in human melanocytic lesions supports an adaptive resistance mechanism of immune escape. *Sci Transl Med.* 2012;4:127r137r.

17. Natarajan A, Mayer AT, Xu L, Reeves RE, Gano J, Gambhir SS. Novel radiotracer for immunoPET imaging of PD-1 checkpoint expression on tumor infiltrating lymphocytes. *Bioconjug Chem.* 2015;26:2062–2069. doi:10.1021/acs.bioconjchem.5b00318
18. Ritprajak P, Azuma M. Intrinsic and extrinsic control of expression of the immunoregulatory molecule PD-L1 in epithelial cells and squamous cell carcinoma. *Oral Oncol.* 2015;51:221–228. doi:10.1016/j.oraloncology.2014.11.014
19. Alborelli I, Leonards K, Rothschild SI, et al. Tumor mutational burden assessed by targeted NGS predicts clinical benefit from immune checkpoint inhibitors in non-small cell lung cancer. *J Pathol.* 2020;250:19–29. doi:10.1002/path.5344
20. Shia J. Immunohistochemistry versus microsatellite instability testing for screening colorectal cancer patients at risk for hereditary nonpolyposis colorectal cancer syndrome. Part I. The utility of immunohistochemistry. *J Mol Diagn.* 2008;10:293–300. doi:10.2353/jmoldx.2008.080031
21. Vasen HF, Moslein G, Alonso A, et al. Recommendations to improve identification of hereditary and familial colorectal cancer in Europe. *Fam Cancer.* 2010;9:109–115. doi:10.1007/s10689-009-9291-3
22. Jeantet M, Tougeron D, Tachon G, et al. High intra- and inter-tumoral heterogeneity of RAS mutations in colorectal cancer. *Int J Mol Sci.* 2016;17.
23. Chapusot C, Martin L, Bouvier AM, et al. Microsatellite instability and intratumoural heterogeneity in 100 right-sided sporadic colon carcinomas. *Br J Cancer.* 2002;87:400–404. doi:10.1038/sj.bjc.6600474
24. Matos I, Martin-Liberal J, Garcia-Ruiz A, et al. Capturing hyperprogressive disease with immune-checkpoint inhibitors using RECIST 1.1 criteria. *Clin Cancer Res.* 2020;26:1846–1855. doi:10.1158/1078-0432.CCR-19-2226
25. Champiat S, Lambotte O, Barreau E, et al. Management of immune checkpoint blockade dysimmune toxicities: a collaborative position paper. *Ann Oncol.* 2016;27:559–574. doi:10.1093/annonc/mdv623
26. Daud AI, Wolchok JD, Robert C, et al. Programmed death-ligand 1 expression and response to the anti-programmed death 1 antibody pembrolizumab in melanoma. *J Clin Oncol.* 2016;34:4102–4109. doi:10.1200/JCO.2016.67.2477
27. Balar AV, Galsky MD, Rosenberg JE, et al. Atezolizumab as first-line treatment in cisplatin-ineligible patients with locally advanced and metastatic urothelial carcinoma: a single-arm, multicentre, phase 2 trial. *Lancet.* 2017;389:67–76. doi:10.1016/S0140-6736(16)32455-2
28. Chiou VL, Burotto M. Pseudoprogression and immune-related response in solid tumors. *J Clin Oncol.* 2015;33:3541–3543. doi:10.1200/JCO.2015.61.6870
29. Champiat S, Derle L, Ammari S, et al. Hyperprogressive disease is a new pattern of progression in cancer patients treated by Anti-PD-1/PD-L1. *Clin Cancer Res.* 2017;23:1920–1928. doi:10.1158/1078-0432.CCR-16-1741
30. Maute RL, Gordon SR, Mayer AT, et al. Engineering high-affinity PD-1 variants for optimized immunotherapy and immuno-PET imaging. *Proc Natl Acad Sci U S A.* 2015;112:E6506E6514. doi:10.1073/pnas.1519623112
31. Hettich M, Braun F, Bartholoma MD, Schirmbeck R, Niedermann G. High-resolution PET imaging with therapeutic antibody-based PD-1/PD-L1 checkpoint tracers. *Theranostics.* 2016;6:1629–1640. doi:10.7150/thno.15253
32. Lesniak WG, Chatterjee S, Gabrielson M, et al. PD-L1 detection in tumors using [(64) Cu]Atezolizumab with PET. *Bioconjug Chem.* 2016;27:2103–2110. doi:10.1021/acs.bioconjchem.6b00348
33. England CG, Ehlerding EB, Hernandez R, et al. Preclinical pharmacokinetics and biodistribution studies of 89Zr-labeled pembrolizumab. *J Nucl Med.* 2017;58:162–168. doi:10.2967/jnumed.116.177857
34. Chatterjee S, Lesniak WG, Miller MS, et al. Rapid PD-L1 detection in tumors with PET using a highly specific peptide. *Biochem Biophys Res Commun.* 2017;483:258–263. doi:10.1016/j.bbrc.2016.12.156
35. Mayer AT, Natarajan A, Gordon SR, et al. Practical immuno-PET radiotracer design considerations for human immune checkpoint imaging. *J Nucl Med.* 2017;58:538–546. doi:10.2967/jnumed.116.177659
36. Deng L, Liang H, Burnette B, et al. Irradiation and anti-PD-L1 treatment synergistically promote antitumor immunity in mice. *J Clin Invest.* 2014;124:687–695. doi:10.1172/JCI67313
37. Kikuchi M, Clump DA, Srivastava RM, et al. Preclinical immunoPET/CT imaging using Zr-89-labeled anti-PD-L1 monoclonal antibody for assessing radiation-induced PD-L1 upregulation in head and neck cancer and melanoma. *Oncoimmunology.* 2017;6:e1329071. doi:10.1080/2162402X.2017.1329071
38. Cole EL, Kim J, Donnelly DJ, et al. Radiosynthesis and preclinical PET evaluation of (89) Zr-nivolumab (BMS-936558) in healthy non-human primates. *Bioorg Med Chem.* 2017;25:5407–5414.
39. Gonzalez TD, Meng X, McQuade P, et al. In vivo imaging of the programmed death ligand 1 by (18) F PET. *J Nucl Med.* 2017;58:1852–1857. doi:10.2967/jnumed.117.191718
40. Natarajan A, Patel CB, Habte F, Gambhir SS. Dosimetry prediction for clinical translation of (64) Cu-Pembrolizumab immunoPET targeting human PD-1 expression. *Sci Rep.* 2018;8:633. doi:10.1038/s41598-017-19123-x
41. Truillet C, Oh HLJ, Yeo SP, et al. Imaging PD-L1 expression with immunoPET. *Bioconjug Chem.* 2018;29(1):96–103. doi:10.1021/acs.bioconjchem.7b00631
42. Donnelly DJ, Smith RA, Morin P, et al. Synthesis and biologic evaluation of a novel (18) f-labeled adnectin as a PET radioligand for imaging PD-L1 expression. *J Nucl Med.* 2018;59:529–535. doi:10.2967/jnumed.117.199596
43. Li D, Cheng S, Zou S, et al. Immuno-PET Imaging of (89) Zr Labeled Anti-PD-L1 Domain Antibody. *Mol Pharm.* 2018;15:1674–1681. doi:10.1021/acs.molpharmaceut.8b00062
44. De Silva RA, Kumar D, Lisok A, et al. Peptide-Based (68) Ga-PET Radiotracer for Imaging PD-L1 expression in cancer. *Mol Pharm.* 2018;15:3946–3952. doi:10.1021/acs.molpharmaceut.8b00399
45. Moroz A, Lee CY, Wang YH, et al. A preclinical assessment of (89) Zr-atezolizumab identifies a requirement for carrier added formulations not observed with (89) Zr-C4. *Bioconjug Chem.* 2018;29:3476–3482. doi:10.1021/acs.bioconjchem.8b00632
46. Niemeijer AN, Leung D, Huisman MC, et al. Whole body PD-1 and PD-L1 positron emission tomography in patients with non-small-cell lung cancer. *Nat Commun.* 2018;9:4664.
47. Bensch F, van der Veen EL, Lub-de HM, et al. (89) Zr-atezolizumab imaging as a non-invasive approach to assess clinical response to PD-L1 blockade in cancer. *Nat Med.* 2018;24:1852–1858. doi:10.1038/s41591-018-0255-8
48. Li D, Zou S, Cheng S, Song S, Wang P, Zhu X. Monitoring the response of PD-L1 expression to epidermal growth factor receptor tyrosine kinase inhibitors in nonsmall-cell lung cancer xenografts by immuno-PET imaging. *Mol Pharm.* 2019;16:3469–3476. doi:10.1021/acs.molpharmaceut.9b00307
49. Ehlerding EB, Lee HJ, Barnhart TE, et al. Noninvasive imaging and quantification of radiotherapy-induced PD-L1 Upregulation with (89) Zr-Df-Atezolizumab. *Bioconjug Chem.* 2019;30:1434–1441. doi:10.1021/acs.bioconjchem.9b00178
50. Lv G, Sun X, Qiu L, et al. PET imaging of Tumor PD-L1 expression with a highly specific nonblocking single-domain antibody. *J Nucl Med.* 2020;61:117–122. doi:10.2967/jnumed.119.226712

51. Christensen C, Kristensen LK, Alfsen MZ, Nielsen CH, Kjaer A. Quantitative PET imaging of PD-L1 expression in xenograft and syngeneic tumour models using a site-specifically labelled PD-L1 antibody. *Eur J Nucl Med Mol Imaging*. 2020;47:1302–1313. doi:10.1007/s00259-019-04646-4
52. Heskamp S, Hobo W, Molkenboer-Kueneen JD, et al. Noninvasive imaging of tumor PD-L1 expression using radiolabeled Anti-PD-L1 antibodies. *Cancer Res*. 2015;75:2928–2936. doi:10.1158/0008-5472.CAN-14-3477
53. Josefsson A, Nedrow JR, Park S, et al. Imaging, biodistribution, and dosimetry of radionuclide-labeled PD-L1 antibody in an immunocompetent mouse model of breast cancer. *Cancer Res*. 2016;76:472–479. doi:10.1158/0008-5472.CAN-15-2141
54. Garcia MF, Zhang X, Shah M, et al. (99m) Tc-bioorthogonal click chemistry reagent for in vivo pretargeted imaging. *Bioorg Med Chem*. 2016;24:1209–1215. doi:10.1016/j.bmc.2016.01.046
55. Nedrow JR, Josefsson A, Park S, Ranka S, Roy S, Sgouros G. Imaging of programmed cell death ligand 1: impact of protein concentration on distribution of anti-PD-L1 SPECT agents in an immunocompetent murine model of melanoma. *J Nucl Med*. 2017;58:1560–1566. doi:10.2967/jnumed.117.193268
56. Heskamp S, Wierstra PJ, Molkenboer-Kueneen J, et al. PD-L1 microSPECT/CT imaging for longitudinal monitoring of PD-L1 expression in syngeneic and humanized mouse models for cancer. *Cancer Immunol Res*. 2019;7:150–161. doi:10.1158/2326-6066.CIR-18-0280
57. Qiu L, Tan H, Lin Q, et al. A pretargeted imaging strategy for immune checkpoint ligand PD-L1 expression in tumor based on bioorthogonal diels-alder click chemistry. *Mol Imaging Biol*. 2019.
58. Xing Y, Chand G, Liu C, et al. Early phase I study of a (99m) Tc-labeled anti-programmed death ligand-1 (PD-L1) single-domain antibody in SPECT/CT assessment of PD-L1 expression in non-small cell lung cancer. *J Nucl Med*. 2019;60:1213–1220. doi:10.2967/jnumed.118.224170
59. Fay AP, Signoretti S, Callea M, et al. Programmed death ligand-1 expression in adrenocortical carcinoma: an exploratory biomarker study. *J Immunother Cancer*. 2015;17:3:3.
60. Du Y, Sun T, Liang X, et al. Improved resection and prolonged overall survival with PD-1-IRDye800CW fluorescence probe-guided surgery and PD-1 adjuvant immunotherapy in 4T1 mouse model. *Int J Nanomedicine*. 2017;12:8337–8351. doi:10.2147/IJN.S149235
61. Ke X, Lin W, Li X, Wang H, Xiao X, Guo Z. DRUG DELIVERY. *Nanoscale*. 2016;8:12618–12625.
62. Du Y, Liang X, Li Y, et al. (2017) Liposomal nanohybrid cerasomes targeted to PD-L1 enable dual-modality imaging and improve antitumor treatments. *Cancer Lett*. 2018;414:230–238.
63. Du Y, Liang X, Li Y, et al. Nuclear and Fluorescent Labeled PD-1-Liposome-DOX-<sup>64</sup>Cu/IRDye800CW allows improved breast tumor targeted imaging and therapy. *Mol Pharm*. 2017;14(11):3978–3986. doi:10.1021/acs.molpharmaceut.7b00649
64. Tazdait M, Mezquita L, Lahmar J, et al. Patterns of responses in metastatic NSCLC during PD-1 or PDL-1 inhibitor therapy: comparison of RECIST 1.1, irRECIST and iRECIST criteria. *Eur J Cancer*. 2018;88:38–47. doi:10.1016/j.ejca.2017.10.017
65. Wolchok JD, Hoos A, O'Day S. Guidelines for the evaluation of immune therapy activity in solid tumors: immune-related response criteria. *Clin Cancer Res*. 2009;15:7412–7420. doi:10.1158/1078-0432.CCR-09-1624
66. Topalian SL, Sznol M, McDermott DF, et al. Survival, durable tumor remission, and long-term safety in patients with advanced melanoma receiving nivolumab. *J Clin Oncol*. 2014;32:1020–1030. doi:10.1200/JCO.2013.53.0105
67. Hodi FS, Hwu WJ, Kefford R, et al. Evaluation of immune-related response criteria and RECIST v1.1 in patients with advanced melanoma treated with pembrolizumab. *J Clin Oncol*. 2016;34:1510–1517. doi:10.1200/JCO.2015.64.0391
68. Wolchok JD, Kluger H, Callahan MK, et al. Nivolumab plus ipilimumab in advanced melanoma. *N Engl J Med*. 2013;369:122–133. doi:10.1056/NEJMoa1302369
69. Miller AB, Hoogstraten B, Staquet M, Winkler A. Reporting results of cancer treatment. *Cancer-Am Cancer Soc*. 1981;47:207–214.
70. Therasse P, Arbuck SG, Eisenhauer EA, et al. New guidelines to evaluate the response to treatment in solid tumors. European Organization for Research and Treatment of Cancer, National Cancer Institute of the United States, National Cancer Institute of Canada. *J Natl Cancer Inst*. 2000;92:205–216. doi:10.1093/jnci/92.3.205
71. Eisenhauer EA, Therasse P, Bogaerts J, et al. New response evaluation criteria in solid tumours: revised RECIST guideline (version 1.1). *Eur J Cancer*. 2009;45:228–247. doi:10.1016/j.ejca.2008.10.026
72. Wahl RL, Jacene H, Kasamon Y, Lodge MA. From RECIST to PERCIST: evolving Considerations for PET response criteria in solid tumors. *J Nucl Med*. 2009;50(Suppl 1):122S150S. doi:10.2967/jnumed.108.057307
73. Beer L, Hochmair M, Haug AR, et al. Comparison of RECIST, iRECIST, and PERCIST for the evaluation of response to PD-1/PD-L1 blockade therapy in patients with non-small cell lung cancer. *Clin Nucl Med*. 2019;44:535–543. doi:10.1097/RLU.0000000000002603
74. Kaira K, Higuchi T, Naruse I, et al. Metabolic activity by (18) F-FDG-PET/CT is predictive of early response after nivolumab in previously treated NSCLC. *Eur J Nucl Med Mol Imaging*. 2018;45:56–66. doi:10.1007/s00259-017-3806-1
75. Cho SY, Lipson EJ, Im HJ, et al. Prediction of response to immune checkpoint inhibitor therapy using early-time-point (18) F-FDG PET/CT imaging in patients with advanced melanoma. *J Nucl Med*. 2017;58:1421–1428. doi:10.2967/jnumed.116.188839
76. Higuchi M, Owada Y, Inoue T, et al. FDG-PET in the evaluation of response to nivolumab in recurrent non-small-cell lung cancer. *World J Surg Oncol*. 2016;14:238. doi:10.1186/s12957-016-0998-y
77. Sachpekidis C, Larribere L, Pan L, Haberkorn U, Dimitrakopoulou-Strauss A, Hassel JC. Predictive value of early 18F-FDG PET/CT studies for treatment response evaluation to ipilimumab in metastatic melanoma: preliminary results of an ongoing study. *Eur J Nucl Med Mol Imaging*. 2015;42:386–396. doi:10.1007/s00259-014-2944-y
78. Tan AC, Emmett L, Lo S, et al. FDG-PET response and outcome from anti-PD-1 therapy in metastatic melanoma. *Ann Oncol*. 2018;29:2115–2120. doi:10.1093/annonc/mdy330
79. Ito K, Teng R, Schoder H, et al. (18) F-FDG PET/CT for monitoring of ipilimumab therapy in patients with metastatic melanoma. *J Nucl Med*. 2019;60:335–341. doi:10.2967/jnumed.118.213652
80. Ito K, Schoder H, Teng R, et al. Prognostic value of baseline metabolic tumor volume measured on (18) F-fluorodeoxyglucose positron emission tomography/computed tomography in melanoma patients treated with ipilimumab therapy. *Eur J Nucl Med Mol Imaging*. 2019;46:930–939. doi:10.1007/s00259-018-4211-0
81. Rossi G, Bauckneht M, Genova C, et al. Comparison between 18F-FDG-PET- and CT-based criteria in non-small cell lung cancer (NSCLC) patients treated with Nivolumab. *J Nucl Med*. 2019.
82. Annovazzi A, Vari S, Giannarelli D, et al. Comparison of 18F-FDG PET/CT criteria for the prediction of therapy response and clinical outcome in patients with metastatic melanoma treated with ipilimumab and PD-1 Inhibitors. *Clin Nucl Med*. 2020;45:187–194. doi:10.1097/RLU.0000000000002921
83. Dercle L, Seban RD, Lazarovici J, et al. (18) F-FDG PET and CT scans detect new imaging patterns of response and progression in patients with hodgkin lymphoma treated by anti-programmed death 1 immune checkpoint inhibitor. *J Nucl Med*. 2018;59:15–24. doi:10.2967/jnumed.117.193011

84. Lim I, Lindenberg ML, Mena E, et al. (18) F-Sodium fluoride PET/CT predicts overall survival in patients with advanced genitourinary malignancies treated with cabozantinib and nivolumab with or without ipilimumab. *Eur J Nucl Med Mol Imaging*. 2020;47:178–184. doi:10.1007/s00259-019-04483-5
85. Weber JS, Hodi FS, Wolchok JD, et al. Safety profile of nivolumab monotherapy: a pooled analysis of patients with advanced melanoma. *J Clin Oncol*. 2017;35:785–792.
86. Wang DY, Salem JE, Cohen JV, et al. Fatal toxic effects associated with immune checkpoint inhibitors: a systematic review and meta-analysis. *Jama Oncol*. 2018;4:1721–1728. doi:10.1001/jamaoncol.2018.3923
87. Mekki A, Derclé L, Lichtenstein P, et al. Detection of immune-related adverse events by medical imaging in patients treated with anti-programmed cell death 1. *Eur J Cancer*. 2018;96:91–104. doi:10.1016/j.ejca.2018.03.006
88. Weber JS, Kahler KC, Hauschild A. Management of immune-related adverse events and kinetics of response with ipilimumab. *J Clin Oncol*. 2012;30:2691–2697. doi:10.1200/JCO.2012.41.6750
89. Wachsmann JW, Ganti R, Peng F. Immune-mediated Disease in Ipilimumab Immunotherapy of Melanoma with FDG PET-CT. *Acad Radiol*. 2017;24:111–115. doi:10.1016/j.acra.2016.08.005
90. Rajabian Z, Kalani F, Taghilloo S, et al. Over-expression of immunosuppressive molecules, PD-L1 and PD-L2, in ulcerative colitis patients. *Iran J Immunol*. 2019;16:62–70.
91. Buchbinder E, Hodi FS. Cytotoxic T lymphocyte antigen4 and immune checkpoint blockade. *J Clin Invest*. 2015;125:3377–3383. doi:10.1172/JCI80012
92. Higashikawa K, Yagi K, Watanabe K, et al. 64Cu-DOTA-anti-CTLA-4 mAb enabled PET visualization of CTLA-4 on the T-cell infiltrating tumor tissues. *PLoS One*. 2014;9(11):e109866. doi:10.1371/journal.pone.0109866
93. Ehlerding EB, England CG, Majewski RL, et al. ImmunoPET imaging of CTLA-4 expression in mouse models of non-small cell lung cancer. *Mol Pharm*. 2017;14(5):1782–1789. doi:10.1021/acs.molpharmaceut.7b00056
94. Ehlerding EB, Lee HJ, Jiang D, et al. Antibody and fragment-based PET imaging of CTLA-4+T-cells in humanized mouse models. *Am J Cancer Res*. 2019;9(1):53–63.
95. Voskoboinik I, Whisstock JC, Trapani JA. Perforin and granzymes: function, dysfunction and human pathology. *Nat Rev Immunol*. 2015;15(6):388–400. doi:10.1038/nri3839
96. Larimer BM, Wehrenberg-Klee E, Dubois F, et al. Granzyme B PET imaging as a predictive biomarker of immunotherapy response. *Cancer Res*. 2017;77(9):2318–2327.
97. Schoenborn JR, Wilson CB. Regulation of interferon-gamma during innate and adaptive immune responses. *Adv Immunol*. 2007;96:41–101.
98. Coussens LM, Zitvogel L, Palucka AK. Neutralizing tumor-promoting chronic inflammation: a magic bullet? [published correction appears in *Science*. 2013;339(6117):286–291.
99. Kovács T, Mikó E, Ujlaki G, Sári Z, Bai P. The microbiome as a component of the tumor microenvironment. *Adv Exp Med Biol*. 2020;1225:137–153.
100. Knutson KL, Disis ML. Tumor antigen-specific T helper cells in cancer immunity and immunotherapy. *Cancer Immunol Immunother*. 2005;54(8):721–728. doi:10.1007/s00262-004-0653-2
101. Xu X, Fu XY, Plate J, Chong AS. IFN-gamma induces cell growth inhibition by Fas-mediated apoptosis: requirement of STAT1 protein for up-regulation of Fas and FasL expression. *Cancer Res*. 1998;58(13):2832–2837.
102. Zaidi MR, Merlino G. The two faces of interferon- $\gamma$  in cancer. *Clin Cancer Res*. 2011;17(19):6118–6124. doi:10.1158/1078-0432.CCR-11-0482
103. Gibson HM, McKnight BN, Malysa A, et al. IFN $\gamma$  PET imaging as a predictive tool for monitoring response to tumor immunotherapy. *Cancer Res*. 2018;78(19):5706–5717. doi:10.1158/0008-5472.CAN-18-0253
104. Gooden MJM, De Bock GH, Leffers N, Daemen T, Nijman HW. The prognostic influence of tumour-infiltrating lymphocytes in cancer: a systematic review with meta-analysis. *Br J Cancer*. 2011;105:93–103. doi:10.1038/bjc.2011.189
105. Tumei PC, Harview CL, Yearley JH, et al. PD-1 blockade induces responses by inhibiting adaptive immune resistance. *Nature*. 2014;515:568–571. doi:10.1038/nature13954
106. Hadrup S, Donia M, Thor Straten P. Effector CD4 and CD8 T cells and their role in the tumor microenvironment. *Cancer Microenviron*. 2013;6:123–133. doi:10.1007/s12307-012-0127-6
107. Fridman WH, Pagès F, Sautès-Fridman C, Galon J. The immune contexture in human tumours: impact on clinical outcome. *Nat Rev Cancer*. 2012;12:298–306.
108. Gentles AJ, Newman AM, Liu CL, et al. The prognostic landscape of genes and infiltrating immune cells across human cancers. *Nat Med*. 2015;21:938–945. doi:10.1038/nm.3909
109. Galon J, Costes A, Sanchez-Cabo F, et al. Type, density, and location of immune cells within human colorectal tumors predict clinical outcome. *Science*. 2006;313:1960–1964. doi:10.1126/science.1129139
110. Tavaré R, McCracken MN, Zettlitz KA, et al. Engineered antibody fragments for immuno-PET imaging of endogenous CD8+ T cells in vivo. *Proc Natl Acad Sci U S A*. 2014;111(3):1108–1113. doi:10.1073/pnas.1316922111
111. Tavaré R, McCracken MN, Zettlitz KA, et al. Immuno-PET of Murine T cell reconstitution postadoptive stem cell transplantation using anti-CD4 and Anti-CD8 Cys-Diabodies. *J Nucl Med*. 2015;56(8):1258–1264. doi:10.2967/jnumed.114.153338
112. Tavaré R, Escuin-Ordinas H, Mok S, et al. An effective immuno-pet imaging method to monitor cd8-dependent responses to immunotherapy. *Cancer Res*. 2016;76(1):73–82. doi:10.1158/0008-5472.CAN-15-1707
113. Kristensen LK, Fröhlich C, Christensen C, et al. CD4+ and CD8a+ PET imaging predicts response to novel PD-1 checkpoint inhibitor: studies of Sym021 in syngeneic mouse cancer models. *Theranostics*. 2019;9(26):8221–8238. doi:10.7150/thno.37513
114. Pandit-Taskar N, Postow MA, Hellmann MD, et al. First-in-humans imaging with 89Zr-Df-IAB22M2C Anti-CD8 minibody in patients with solid malignancies: preliminary pharmacokinetics, biodistribution, and lesion targeting. *J Nucl Med*. 2020;61(4):512–519. doi:10.2967/jnumed.119.229781
115. Willoughby J, Griffiths J, Tews I, Cragg MS. OX40: structure and function – what questions remain? *Mol Immunol*. 2017;83:13–22. doi:10.1016/j.molimm.2017.01.006
116. Alam IS, Mayer AT, Sagiv-Barfi I, et al. Imaging activated T cells predicts response to cancer vaccines. *J Clin Invest*. 2018;128(6):2569–2580. doi:10.1172/JCI98509
117. Nabergoj S, Mlinarič-Raščan I, Jakopin Ž. Harnessing the untapped potential of nucleotide-binding oligomerization domain ligands for cancer immunotherapy. *Med Res Rev*. 2019;39(5):1447–1484.
118. Kapp K, Volz B, Curran MA, Oswald D, Wittig B, Schmidt M. EnanDIM - a novel family of L-nucleotide-protected TLR9 agonists for cancer immunotherapy. *J Immunother Cancer*. 2019;7(1):5. doi:10.1186/s40425-018-0470-3

## Cancer Management and Research

Dovepress

### Publish your work in this journal

Cancer Management and Research is an international, peer-reviewed open access journal focusing on cancer research and the optimal use of preventative and integrated treatment interventions to achieve improved outcomes, enhanced survival and quality of life for the cancer patient.

The manuscript management system is completely online and includes a very quick and fair peer-review system, which is all easy to use. Visit <http://www.dovepress.com/testimonials.php> to read real quotes from published authors.

Submit your manuscript here: <https://www.dovepress.com/cancer-management-and-research-journal>